Spatial and Temporal Integration Abnormalities in X-Linked Retinoschisis

J. Jason McAnany,[1,2] Jason C. Park,[1] Gerald A. Fishman,[1,3] and Robert A. Hyde[1]

[1]Department of Ophthalmology and Visual Sciences, University of Illinois at Chicago, Chicago, Illinois, United States
[2]Department of Bioengineering, University of Illinois at Chicago, Chicago, Illinois, United States
[3]The Pangere Center for Inherited Retinal Diseases, The Chicago Lighthouse, Chicago, Illinois, United States

PURPOSE. To evaluate spatial and temporal integration across the visual field in individuals with juvenile X-linked retinoschisis (XLRS).

METHODS. Nine subjects with XLRS and 10 visually normal individuals participated. Luminance thresholds were measured at 15 locations along the horizontal visual field meridian. Locations were grouped into four regions for analysis: foveal, parafoveal (2°), perifoveal (5°–10°), and peripheral (10°–60°). For spatial integration measurements, stimulus duration was 100 ms, and size ranged from 0.01 to 2.32 deg^2 (Goldmann I–V). For temporal integration measurements, stimulus size was 0.15 deg^2 (Goldmann III), and duration ranged from 12 to 800 ms. The effect of stimulus size and duration on the subjects' threshold was described using integration models.

RESULTS. Luminance thresholds for the XLRS group were more elevated for small targets (2.0×–12.6×) than for large targets (1.25×–3.2×) compared to controls for all locations. Likewise, thresholds for the XLRS group were more elevated for short durations (6.3×) than for long durations (4.0×) in the fovea and parafovea but were similarly elevated at all durations (2.0×–2.5×) in the perifovea and periphery. For both the size and duration experiments, thresholds measured in the fovea, parafovea, and perifovea of XLRS subjects were highly similar to those measured from the peripheral field of the controls.

CONCLUSIONS. Spatial and temporal integration characteristics of the XLRS fovea, parafovea, and perifovea are similar to those of the normal periphery. The results also indicate that scaling stimulus size equates thresholds for the XLRS and control subjects throughout the visual field, but scaling duration does not.

Keywords: X-linked retinoschisis, static perimetry, spatial integration, temporal integration, visual psychophisics

Juvenile X-linked retinoschisis (XLRS) is a non-syndromic, congenital vitreoretinal disease that is estimated to affect 1 in 5000 to 1 in 20,000 males.[1] XLRS is associated with mutations in the *retinoschisin 1* (*RS1*) gene that are inherited as an X-linked recessive trait.[2–4] Affected males often present with cystic-appearing macular lesions, but peripheral retinoschisis is also common.[3] The bilateral foveal schisis that is apparent in young individuals typically collapses with advancing age, proceeding to an atrophic stage. Although foveal thinning and macular atrophy are apparent in older individuals, younger patients can have thinning of the photoreceptor layer,[5,6] suggesting that outer retinal abnormalities may be an early characteristic of the disease in some individuals.

The structural abnormalities that are apparent by fundus examination and optical coherence tomography (OCT) are accompanied by functional deficits, including a loss of visual acuity and abnormal electroretinograms.[1,3,7,8] Tests of visual function including kinetic perimetry,[9–13] static perimery,[10,12,14] microperimetry,[10,15–17] and full-field threshold testing[18] have shown variable extents of abnormality in XLRS. A recent perimetry study examined luminance thresh-olds across the visual field under a broad range of adaptation levels (dark-adapted scotopic conditions to 50 cd/m^2 photopic conditions) in a group of subjects who had XLRS.[6] This study found that the pattern of threshold elevation in XLRS was complex, with the extent of abnormality depending on both the adaptation level and the visual field location tested. Interestingly, thresholds measured in the macula of the XLRS subjects were similar to thresholds measured in the peripheral field of control subjects. This finding generally supports a previous hypothesis[19] that the fovea of subjects with XLRS is functionally similar to the parafoveal retina of visually normal individuals.

As an additional approach to test this hypothesis, spatial and temporal integration can be assessed across the visual field. Classic psychophysical studies of spatial integration involve measuring luminance thresholds for stimuli of different sizes.[20–22] For small stimuli (less than approximately 10 min arc), the relationship between threshold and stimulus size is commonly described by Ricco's size-intensity reciprocity law, which states that log threshold decreases linearly with log stimulus area with a slope of −1.0. For larger targets, log threshold decreases linearly with

log stimulus area with a slope of −0.5 (Piper's law) or −0.33 (Pieron's law). In practice, however, the relationship between threshold and size is well described by a power function that transitions from a slope of −1 to 0, which is applicable across a broad range of stimulus sizes.[22,23] Although spatial summation characteristics have not been reported in subjects with XLRS, there is reason to suspect that thresholds may be more abnormal for small test targets as compared to large test targets. Specifically, previous work has shown that individuals with XLRS have normal, or nearly normal, thresholds for low spatial frequency gratings (equivalent to large stimuli) and that thresholds can be substantially elevated for high spatial frequency gratings (equivalent to small stimuli).[19] This finding is consistent with the loss of visual acuity in XLRS.[1,3,12]

Psychophysical studies of temporal integration involve measuring luminance thresholds for stimuli presented at different durations at a fixed size.[20,24,25] For short stimulus exposure durations (less than approximately 20 ms), the relationship between threshold and stimulus duration conforms to Bloch's time–intensity reciprocity law, which states that log threshold decreases linearly with log stimulus duration with a slope of −1.0.[25] For longer durations, thresholds typically decrease less sharply (slope > −1.0), eventually becoming independent of duration. Consistent with the findings in the spatial domain discussed above,[22,23] the relationship between threshold and stimulus duration is well described by a power function that transitions from a slope of −1 to 0. Although temporal integration characteristics have not been reported in individuals with XLRS, there is reason to suspect that thresholds may be more abnormal at short durations compared to long durations. Specifically, electrophysiological studies have shown that individuals with XLRS have normal response amplitudes elicited by slowly flickering stimuli (below approximately 16 Hz) and substantially attenuated responses for rapidly flickering stimuli (above approximately 30 Hz).[26–28] At present, it is unknown if these electrophysiological findings translate to psychophysically measured behavioral responses.

Building on these previous findings, the purpose of the present study was to measure luminance thresholds to evaluate spatial and temporal integration in individuals who have confirmed *RS1* mutations. Measurements were performed across the visual field to determine how spatial and temporal integration varies as a function of retinal eccentricity in XLRS, as compared to visually normal individuals. These measurements were used to evaluate the hypothesis that the central macula of subjects with XLRS is functionally similar to the peripheral retina of visually normal individuals.

METHODS

Subjects

The tenets of the Declaration of Helsinki were followed, and all procedures were approved by an institutional review board of the University of Illinois at Chicago. Subjects provided written informed consent prior to participating. Nine unrelated male subjects with a diagnosis of XLRS (ages 18–49 years) were recruited from the cohorts of the Chicago Lighthouse and the Illinois Eye and Ear Infirmary at the University of Illinois. The diagnosis of XLRS was based on characteristic fundus features, including a spoke wheel pattern of macular schisis, cystic-appearing macular lesions on OCT, and functional abnormalities including visual acuity loss and a reduced electroretinogram b/a amplitude ratio. Each individual had a mutation in the *RS1* gene. The Table lists the age, visual acuity, refractive error, *RS1* mutation, XLRS categorization, and carbonic anhydrase inhibitor use for each subject at the time of testing. The XLRS categorization is based on structural abnormalities that were observed on fundus examination and by OCT imaging as originally described by Prenner et al.[29] and expanded upon by Lesch et al.[30] Details of the categorization are provided in Supplementary Table S1. An OCT image (b-scan through the fovea) is provided for each XLRS subject in Supplementary Figure S1. In addition, Supplementary Figure S1 provides eye tracking data obtained with a microperimeter[31] showing that each XLRS subject had stable fixation and that eight of the nine subjects fixated with the anatomical fovea (see Supplementary Materials for details).

Ten visually normal control subjects (six male and four female; ages 23–42 years) with no history of eye disease, Early Treatment Diabetic Retinopathy Study best-corrected visual acuity of 0 logMAR or better, and normal contrast sensitivity assessed with the Pelli–Robson chart also participated in the study. There was no significant difference between the mean ages of the control group (29 years) and the XLRS group (31 years; $t = 0.40$, $P = 0.69$). Although previous work indicates sex differences in some psychophysical tasks,[32] there were no apparent threshold differences in the present sample of male and female control subjects. These XLRS and control subjects participated in a comprehensive evaluation of psychophysical function, in which thresholds were measured under different adaptation conditions, in the presence of visual luminance noise, and for stimuli of different size and duration. The present study reports the spatial and temporal integration data; the adaptation and luminance noise data are presented elsewhere.[6,33] Two subjects (both controls) had prior experience with psychophysical testing.

TABLE. Subject Characteristics

Subject No.	Color Code	Age (y)	Acuity (logMAR)	Refractive Error	*RS1* Variant	XLRS Class	Carbonic Anhydrase Inhibitor Treatment
1	Brown	18	0.52	−2.50 +0.25 ×75	c.214G>A (p.Glu72Lys)	3	Acetazolamide
2	Green	19	0.68	+3.00 +0.75 ×170	c.218C>A (p.Ser73*)	3	No
3	Light blue	21	0.58	0.00 +1.00 ×40	Deletion of exons 1–5	4	No
4	Gray	25	0.36	−1.75 +1.75 ×147	Deletion of exon 2	3	No
5	Pink	34	0.56	+2.25 +2.75 ×25	c.578C>T (p.Pro193Leu)	4	No
6	Black	35	0.60	+1.75 +1.25 ×161	c.422G>A (p.Arg141His)	8	Acetazolamide
7	Blue	37	0.66	+2.00 +0.50 ×15	c.208G>A (p.Gly70Ser)	4	No
8	Red	40	0.40	+4.75 +1.00 ×0	c.208G>A (p.Gly70Ser)	8	No
9	Yellow	49	0.60	−6.00 +1.75 ×0	c.286T>C (p.Trp96Arg)	7	No

Apparatus, Stimuli, and Procedure

All testing was performed with a commercially available Octopus 900 Pro perimeter (Haag-Streit, Köniz, Switzerland). Measurements were performed monocularly, with the fellow eye patched. The test stimuli consisted of achromatic spots of light that were presented at 15 locations along the horizontal meridian of the visual field, from 45° temporal to 60° nasal. The stimuli were presented against an achromatic 50-cd/m² field. For most analyses, the 15 locations were grouped into four regions: foveal (0°), parafoveal field (2°), perifoveal field (5°–10°), and peripheral field (10°–60°). Appropriate refractive correction was used for test targets presented within the central 20° and removed for targets presented more peripherally.

For the spatial integration measurements, the stimulus duration was 100 ms, and size ranged from 0.01 to 2.32 deg² (Goldmann I–V). For the temporal integration measurements, the stimulus size was 0.15 deg² (Goldmann III), and the duration ranged from 12 to 800 ms in seven steps separated by approximately 0.3 log units. Threshold data obtained for different stimulus sizes and durations were described using an exponential function, adapted from classic integration studies.[20–22] The equation for the fits is

$$\log T = \log K_1 + K_2 A^{K_3} \qquad (1)$$

where T is threshold; K_1, K_2, and K_3 are constants; and A is the area of the stimulus (deg²). For the temporal summation data, A is replace by the stimulus duration (ms). As discussed by Smith et al.,[23] the exponential fit emphasizes a continual decline in slope, which is more characteristic of the pattern of data, as compared to joining several linear segments predicted by the Ricco, Piper, and Pieron laws. As discussed below, spatial integration measurements for the controls did not conform to Ricco's law in the fovea and parafovea. This is a common finding for measurements performed with standard Goldmann target sizes, which are typically too large to accurately estimate the critical area of spatial integration in and around the fovea.[34,35] Given the limitations imposed by the use of standard Goldmann target sizes, Equation 1 was used to describe spatial and temporal integration, rather forcing a two-limb linear regression fit with an initial slope of −1 to the data.

Results

Figure 1 plots the mean log thresholds (±SEM) along the horizontal meridian for the control subjects (left) and XLRS subjects (right). Each function was obtained with a different stimulus size, as indicated to the right (Goldmann I–V). The pattern of control data appears V-shaped, with thresholds decreasing from the periphery to the fovea for all stimulus sizes. The V-shape is sharper for small stimuli compared to large stimuli, indicating a greater effect of location on the threshold for small test targets. In addition, the decrease in thresholds as stimulus size increased was greater in the periphery (size I to V difference of approximately 1.9 log units) compared to the fovea (size I to V difference of approximately 0.8 log units). In contrast, the pattern of thresholds across the horizontal meridian appears W-shaped for the XLRS subjects. That is, thresholds decreased from the periphery toward the fovea, but the fovea/parafovea thresholds tended to be elevated relative to the perifovea. The pattern of thresholds across the meridian is similar for different stimulus sizes, with the size I and size V thresholds differing by approximately 1.7 log units throughout the visual field (uniform vertical shift). Overall, Figure 1 shows two primary differences between the mean XLRS and control functions: (1) thresholds were lowest at the fovea for the control subjects and lowest in the parafovea/perifovea for the XLRS subjects; and (2) spatial integration (change in thresholds with increasing size) was strongly dependent on field location for the controls and weakly dependent on field location for the XLRS subjects.

Figure 2 plots the mean log thresholds (±SEM) as a function of the log stimulus area for the control subjects (black) and XLRS subjects (red). Measurements performed across the visual field were grouped into four regions to simplify visualization (location is indicated in each panel). Data were fit with Equation 1 and are represented by the solid curves. Mean thresholds for the XLRS group were more elevated for small targets (2.0×–12.6×) than for large targets (1.25×–3.2×) compared to the control group for all field locations. Data for individual XLRS subjects are shown in Supplemental Figure S2. Thresholds were approximately similar for the nine subjects with XLRS, with the exception of perifoveal measurement for XLRS subject 2, which were elevated considerably. As shown in Supplemental Figure S1, this subject had a large foveoschisis that extended into the peri-
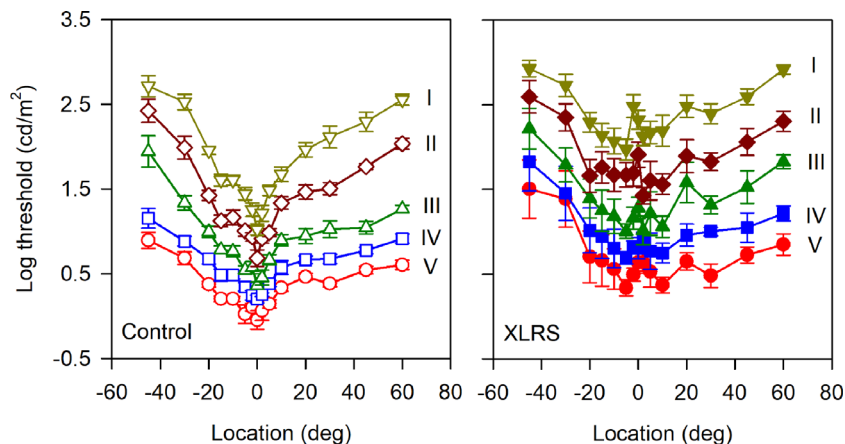
FIGURE 1. Mean (±SEM) log luminance thresholds (cd/m²) measured across the horizontal meridian of the visual field for Goldmann stimulus sizes I to V. Data are shown for the control subjects (*left*) and XLRS subjects (*right*).
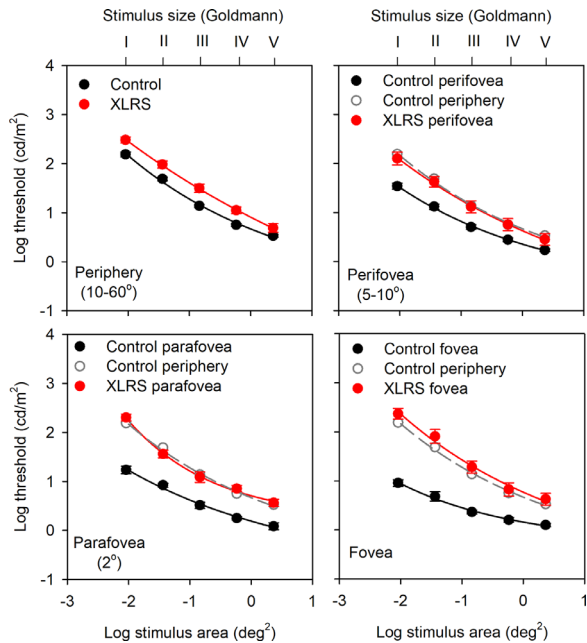
FIGURE 2. Mean (±SEM) log luminance thresholds (cd/m²) are plotted as a function of log stimulus area (equivalent Goldmann sizes are indicated on the upper *x*-axes). Data are shown for the control (*black*) and XLRS (*red*) subjects measured in each of the four visual field regions (periphery, perifovea, parafovea, and fovea). The lines are fits of Equation 1 to the datasets. The data and fit for the control subjects measured in the peripheral visual field are replotted in the perifovea, parafovea, and fovea panels (*open gray circles* and *dashed lines*).

FIGURE 3. Mean thresholds (±SEM) for the control (*black*) and XLRS (*red*) subjects are replotted together from Figure 2. The data from the fovea (*open triangles*), parafovea (*filled triangles*), perifovea (*open circles*), and periphery (*filled circles*) for both subject groups were shifted horizontally along the *x*-axis to align the data into a single function. This function was fit with Equation 1, and the general regions corresponding to Ricco's law, Piper's law, and Pieron's law are marked.

fovea and a disrupted inner segment ellipsoid, which may be related to his elevated perifoveal thresholds. Repeated-measures ANOVA, which was performed to analyze the group differences, indicated significant differences in log thresholds between the control and XLRS subjects within each field location (all $F > 14.31$, $P < 0.002$). The interaction between stimulus size and group was only significant for the peripheral field measurements ($F = 2.59$, $P = 0.044$). Bonferroni-corrected pairwise comparisons indicated significant peripheral field threshold differences between the control and XLRS groups for Goldmann sizes I to IV (all $t > 3.47$, $P < 0.01$), but not for the Goldmann V ($t = 1.89$, $P = 0.07$). Inspection of the data shown in Figure 2 suggests that XLRS thresholds measured in the perifovea, parafovea, and fovea are like those of the normal periphery. To evaluate this further, the control function measured in the periphery was replotted in each of the three other panels (open circles and gray dashed lines). The control data measured in the periphery nearly superimpose upon the XLRS functions measured in the perifovea, parafovea, and fovea. Thresholds measured in the peripheral field of the controls were compared statistically to the thresholds measured in perifovea, parafovea, and fovea of the subjects with XLRS by ANOVA (Fig. 2, red vs. open gray symbols). The analysis indicated no significant threshold differences between the control periphery and the XLRS perifovea, parafovea, or fovea (all $F < 1.39$, $P > 0.25$).

It has been shown that thresholds for stimuli of different spatial frequency (size) can be equated across the visual field in visually normal subjects by scaling the stimulus size.[34,36] To determine if the scaling approach holds for our perimetric thresholds, the control and XLRS data of Figure 2 are
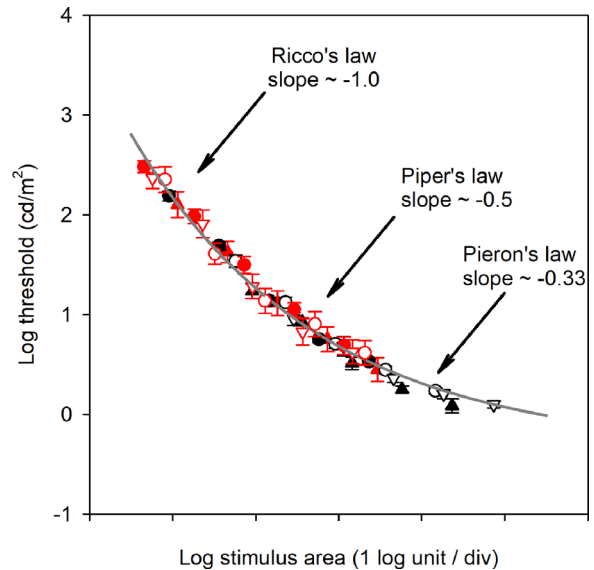
replotted in Figure 3. The thresholds for the control (black) and XLRS (red) subjects were shifted horizontally to form a single function. Shifting the data horizontally along the *x*-axis is equivalent to scaling the stimulus size. The data were fit with Equation 1, with general regions of the Ricco, Piper, and Pieron laws marked. The finding that the data from the control and XLRS subjects form a common function across all field locations indicates that targets for the XLRS and control subjects can be made equally visible by magnifying the stimulus size. For example, to match the mean foveal threshold of the control subjects for a Goldmann I stimulus, the stimulus size for the XLRS subjects at the fovea must be increased to Goldmann IV. To match these thresholds in the parafovea, the mean control stimulus must be increased from size I to size II, whereas the mean XLRS stimulus should be slightly decreased from size IV (falling between sizes III and IV).

Figure 4 plots the mean log thresholds (±SEM) along the horizontal meridian for the control subjects (left) and XLRS subjects (right). Each function was obtained with a different stimulus duration, as indicated in the key. As for the spatial data shown in Figure 1, the threshold–duration functions appear V-shaped for the controls and W-shaped for the XLRS subjects. As stimulus duration increased from 12 to 800 ms, thresholds for the control subjects decreased by 0.7 log units at the fovea and by 1.2 log units in the periphery. By contrast, thresholds for the XLRS subjects decreased by approximately 1.1 log units for all field locations as stimulus duration increased from 12 to 800 ms.

Figure 5 plots the mean log thresholds (±SEM) as a function of the log stimulus area for the control subjects (black) and XLRS subjects (red). Data for individual XLRS subjects are shown in Supplemental Figure S3. Mean thresholds for the XLRS group were somewhat more elevated for short durations (6.3×) than for long durations (4.0×) in the fovea and parafovea and were similarly elevated at
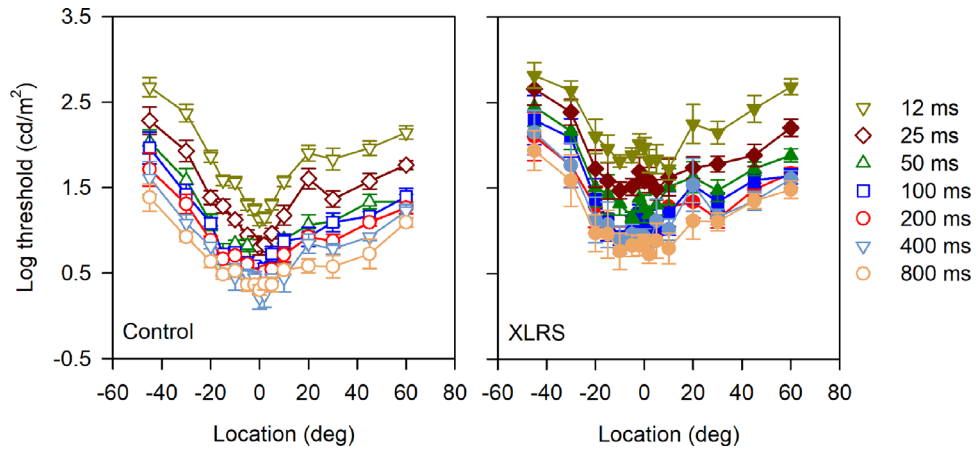
FIGURE 4. Mean (±SEM) log luminance thresholds (cd/m²) measured across the horizontal meridian of the visual field for different stimulus durations (12–800 ms). Data are shown for the control subjects (*left*) and XLRS subjects (*right*).

all durations (2.0×–2.5×) in the perifovea and periphery. Repeated-measures ANOVA indicated significant differences in log thresholds between the control and XLRS subjects within each field location (all $F > 14.38$, $P < 0.002$). The XLRS threshold–duration functions measured in the perifovea, parafovea, and fovea appear like those measured in the peripheral field of the control subjects. This finding is

similar to that observed for the threshold–size functions shown in Figure 2. To evaluate this further, the control function measured in the periphery was replotted in each of the three other panels (Fig. 5, open circles and gray dashed lines). The control data measured in the periphery nearly superimpose upon the XLRS functions measured in the perifovea, parafovea, and fovea. ANOVA indicated no significant
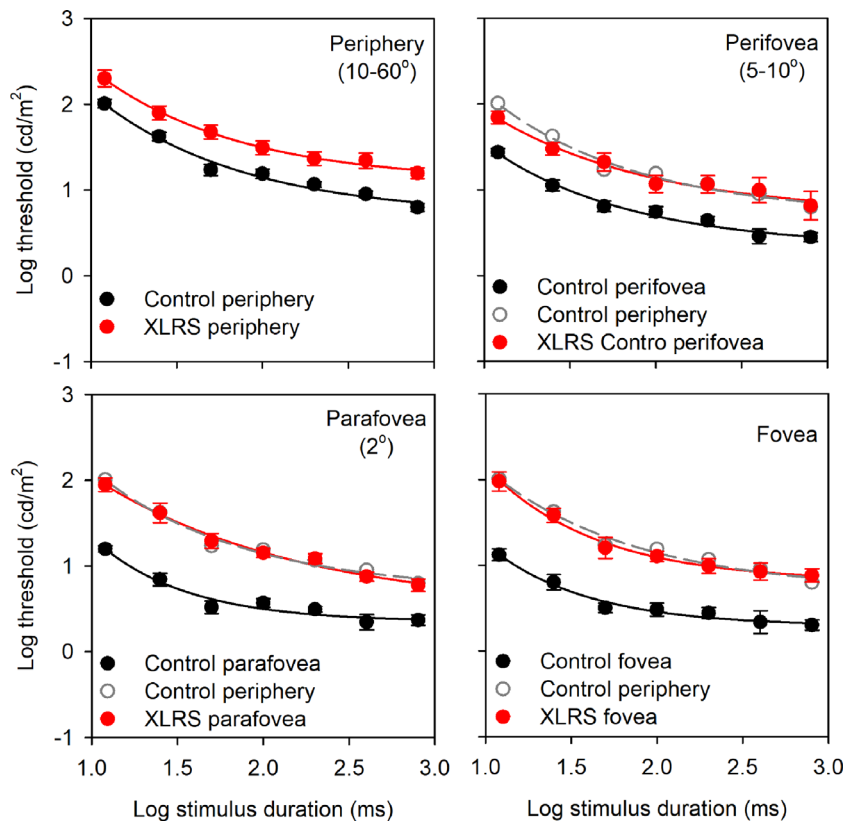

FIGURE 5. Mean (±SEM) log luminance thresholds (cd/m²) are plotted as a function of log stimulus duration. Data are shown for the control (*black*) and XLRS (*red*) subjects measured in each of the four visual field regions (periphery, perifovea, parafovea, and fovea). The lines are fits of Equation 1 to the datasets. The data and fit for the control subjects measured in the peripheral visual field are replotted in the perifovea, parafovea, and fovea panels (*open gray circles* and *dashed lines*).
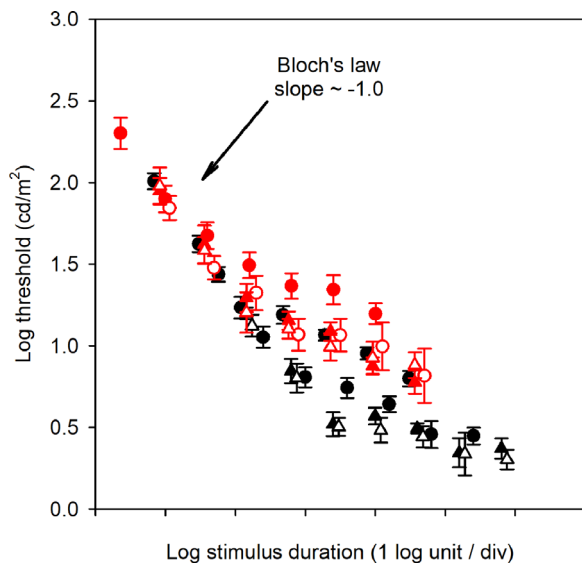
FIGURE 6. Mean thresholds (±SEM) for the control (*black*) and XLRS (*red*) subjects are replotted together from Figure 3. The data for the fovea (*open triangles*), parafovea (*filled triangles*), perifovea (*open circles*), and periphery (*filled circles*) for both subject groups were shifted horizontally along the *x*-axis to align the data into a single function for brief durations. The data failed to align into a single function for moderate to long durations. The general region corresponding to Bloch's law is marked.

threshold differences between the control periphery and the XLRS perifovea, parafovea, or fovea (all $F < 0.20$, $P > 0.66$).

The threshold–duration functions for the control and XLRS subjects (Fig. 5) are replotted together in Figure 6. Thresholds for the control (black) and XLRS (red) subjects for each field location were shifted horizontally to best align the functions at short durations over which Bloch's law generally holds. It is clear from Figure 6 that horizontal shifts, equivalent to scaling the stimulus duration, are not sufficient to align the functions. That is, the functions superimpose in the region in which Bloch's law operates (slope of approximately −1.0) for all subjects in all field locations for these short durations. The threshold–duration functions diverge at longer durations, with the control thresholds being lower than those for the XLRS subjects. This finding is in marked contrast to that of the threshold–size function (Fig. 3), where horizontal shifting aligned the data in a single function. The threshold–duration functions could be aligned to form a uniform function by shifting the data both horizontally and vertically (not shown).

DISCUSSION

This study evaluated luminance thresholds throughout the visual field using stimuli of different size and duration in subjects with XLRS. The primary findings are as follows: (1) XLRS subjects had elevated thresholds for all stimulus sizes, but the abnormality was less for large targets; (2) thresholds for the XLRS subjects at any field location can be equated to the control threshold by scaling the stimulus size; (3) XLRS subjects had elevated thresholds for both long- and short-duration targets for all visual field locations; and (4) thresholds measured in the perifovea, parafovea, and fovea of XLRS subjects were highly similar to thresholds measured in the normal peripheral field.

Although spatial summation across the visual field has not been reported in subjects with XLRS, it has been studied extensively in visually normal individuals[35,37,38] and subjects with glaucoma.[39–41] In visually normal subjects, studies have shown a larger effect of stimulus size in the periphery compared to the fovea, consistent with the control data presented in Figure 1.[35] In contrast, the effect of changing stimulus size was similar throughout the field for the subjects with XLRS. This finding is reflected in the similar functions that relate thresholds and stimulus area for the subjects with XLRS (Fig. 2). That is, the integration functions of Figure 2 were similar throughout the field for the XLRS subjects but differed throughout the field for the control subjects. For the XLRS subjects, the change in log threshold was approximately proportional to the increase in size from Goldmann I to Goldmann II stimulus (slope of −1) throughout the field. This was not the case for the control subjects, who had slopes of approximately −1 in the periphery but not in the perifovea, parafovea, or fovea. Under the specific experimental conditions used in the present study, the traditional Goldmann stimulus sizes did not span a sufficiently broad range to fully map spatial integration (slope of −1 to 0) and accurately quantify the critical area for spatial integration. This is a common limitation of commercially available field perimeters and has been noted in previous work.[34,35]

For the smallest stimulus used in the present study (Goldmann I), individuals with XLRS had threshold elevations, particularly within the central macula, consistent with their contrast sensitivity losses for high spatial frequency gratings.[19] For larger targets (e.g., Goldmann V), mean thresholds for the XLRS subjects were normal in the peripheral field and approached normal at other field locations. A similar pattern was also reported in patients with glaucoma who had greater threshold elevations for small stimuli compared to large stimuli.[39,41] Prior work has also shown that subjects with XLRS maintain relatively good sensitivity for large letter targets,[12,19,33] low spatial frequency gratings,[19] and full-field luminance flashes.[18]

Thresholds for grating stimuli of different spatial frequency can be equated across the visual field in visually normal subjects by scaling the spatial frequency.[36] The present results are consistent with prior work[34,36] showing that scaling stimulus size also equates thresholds across the field for conventional spot stimuli used in visual field perimetry. Specifically, Pan and Swanson[34] concluded that the primary effect of changing eccentricity is to change the spatial scale of the mechanisms mediating detection. In addition, thresholds for stimuli of different sizes presented at different field locations can be matched for visually normal subjects and individuals with XLRS by scaling the stimulus size. For example, a 0.01-deg² stimulus presented at the fovea, a 0.04-deg² stimulus presented in the parafovea, a 0.1-deg² stimulus presented at the perifovea, and a 1.5-deg² stimulus presented in the periphery yielded similar thresholds for the control subjects (10 cd/m²). For the XLRS subjects, this threshold was matched with a foveal stimulus of 0.6 deg², parafoveal and perifoveal stimuli of 0.4 deg², and a peripheral stimulus of 0.6 deg². Indeed, several combinations of stimulus size and location yielded similar thresholds for the control and XLRS subjects.

The characteristics of temporal integration have not been reported in subjects with XLRS. The present study shows that XLRS subjects had elevated thresholds for both long- and short-duration targets measured at all visual field locations. Thresholds for the Goldmann size III stimulus did not

become normal for the longest stimulus durations tested (Fig. 5) and would also be expected to be abnormal for unlimited exposure durations. This results in the need to shift the XLRS threshold–duration functions both horizontally and vertically to align them with the control functions (Fig. 6). This is in contrast to the aforementioned findings in the spatial domain, where thresholds for large targets presented in the periphery were normal for the XLRS subjects, on average, despite their threshold elevations for small targets. Based on previous electrophysiological studies[26–28] showing that amplitude loss was greater for rapid flicker than for slow flicker, it was anticipated that thresholds would be substantially more elevated for short-duration targets than for long-duration targets. This was generally not found. It would be of interest to measure psychophysical thresholds for flickering stimuli in subjects with XLRS, which may provide a more direct comparison to the electrophysiological data obtained with trains of flickering light.[26–28]

Perhaps the most notable finding of the present study is that thresholds measured in the perifovea, parafovea, and fovea of XLRS subjects were highly similar to thresholds measured in the normal peripheral field. This was observed in both the spatial and temporal integration data. This finding supports previous data suggesting that macular function in subjects with XLRS is functionally similar to the peripheral field function of visually normal individuals.[6,19] Specifically, Alexander et al.[19] reported contrast sensitivity and contrast discrimination abnormalities in subjects with XLRS and that the pattern of abnormality in these subjects could be simulated in control observers by testing at a parafoveal locus. The eye tracking data presented in Supplemental Figure S1 that show stable foveal fixation indicate that eccentric viewing does not explain the threshold elevations in the present sample of XLRS subjects. Recently, we reported thresholds across a broad range of adapting levels (scotopic to photopic) in the present group of XLRS subjects.[6] Thresholds were assessed across the visual field and compared to visually normal subjects. The results showed that threshold elevations in XLRS depended on both the adaptation level and the visual field location where the measurement was made. Additionally, the threshold-versus-illuminance relationship observed in the macula of the XLRS subjects was similar to that observed in the peripheral field of the control subjects. Taken together, previous studies, as well as the current dataset, suggest that the receptive field characteristics may be altered in XLRS. A similar conclusion was reached in studies of children with retinopathy of prematurity.[42,43] In these children, integration abnormalities[42–44] may be due to incomplete refinement of receptive fields. As such, receptive field abnormalities may be a common characteristic of diseases that impact the retina early in life.

In summary, photopic luminance thresholds are generally elevated in XLRS relative to visually normal control subjects. The extent of abnormality depends on the location of the stimulus in the visual field, stimulus size, and, to a lesser extent, stimulus duration. The results of both the spatial and temporal integration studies indicate that thresholds measured in the XLRS fovea, parafovea, and perifovea are similar to those measured in the normal periphery. The data also indicate that scaling stimulus size equates thresholds for the XLRS and control subjects throughout the visual field, but scaling duration does not. Overall, these results suggest that receptive field alterations may underlie the threshold elevations in XLRS subjects.

References

1. George ND, Yates JR, Moore AT. X-linked retinoschisis. *Br J Ophthalmol*. 1995;79:697–702.
2. Sauer CG, Gehrig A, Warneke-Wittstock R, et al. Positional cloning of the gene associated with X-linked juvenile retinoschisis. *Nat Genet*. 1997;17:164–170.
3. Sieving PA, MacDonald IM, Chan S. X-linked juvenile retinoschisis. In: Adam MP, Ardinger HH, Pagon RA, et al., eds. *GeneReviews*. Seattle: University of Washington; 1993.
4. Wang T, Zhou A, Waters CT, O'Connor E, Read RJ, Trump D. Molecular pathology of X-linked retinoschisis: mutations interfere with retinoschisin secretion and oligomerisation. *Br J Ophthalmol*. 2006;90:81–86.
5. Bennett LD, Wang YZ, Klein M, Pennesi ME, Jayasundera T, Birch DG. Structure/psychophysical relationships in X-linked retinoschisis. *Invest Ophthalmol Vis Sci*. 2016;57:332–337.
6. McAnany JJ, Park JC, Fishman GA, Hyde RA. Luminance thresholds and their correlation with retinal structure in X-linked retinoschisis. *Invest Ophthalmol Vis Sci*. 2021;62:25.
7. Roesch MT, Ewing CC, Gibson AE, Weber BH. The natural history of X-linked retinoschisis. *Can J Ophthalmol*. 1998;33:149–158.
8. Hahn LC, van Schooneveld MJ, Wesseling NL, et al. X-linked retinoschisis: novel clinical observations and genetic spectrum in 340 patients. *Ophthalmology*. 2022;129:191–202.
9. Apushkin MA, Fishman GA, Rajagopalan AS. Fundus findings and longitudinal study of visual acuity loss in patients with X-linked retinoschisis. *Retina*. 2005;25:612–618.
10. Duncan JL, Ratnam K, Birch DG, et al. Abnormal cone structure in foveal schisis cavities in X-linked retinoschisis from mutations in exon 6 of the *RS1* gene. *Invest Ophthalmol Vis Sci*. 2011;52:9614–9623.
11. Kjellstrom S, Vijayasarathy C, Ponjavic V, Sieving PA, Andreasson S. Long-term 12 year follow-up of X-linked congenital retinoschisis. *Ophthalmic Genet*. 2010;31:114–125.
12. Pennesi ME, Birch DG, Jayasundera KT, et al. Prospective evaluation of patients with X-linked retinoschisis during 18 months. *Invest Ophthalmol Vis Sci*. 2018;59:5941–5956.
13. Collison FT, Fishman GA. Structural and functional monitoring of extramacular cystoid spaces in a case of X-linked retinoschisis treated with acetazolamide. *Retin Cases Brief Rep*. 2018;12:318–321.
14. Peachey NS, Fishman GA, Derlacki DJ, Brigell MG. Psychophysical and electroretinographic findings in X-linked juvenile retinoschisis. *Arch Ophthalmol*. 1987;105:513–516.
15. Jeffrey BG, Cukras CA, Vitale S, Turriff A, Bowles K, Sieving PA. Test-retest intervisit variability of functional and structural parameters in X-linked retinoschisis. *Transl Vis Sci Technol*. 2014;3:5.

16. Bagdonaite-Bejarano L, Hansen RM, Fulton AB. Microperimetry in three inherited retinal disorders. *Semin Ophthalmol*. 2019;34:334–339.

17. Cukras C, Wiley HE, Jeffrey BG, et al. Retinal *AAV8-RS1* gene therapy for X-linked retinoschisis: initial findings from a phase I/IIa trial by intravitreal delivery. *Mol Ther*. 2018;26:2282–2294.

18. McAnany JJ, Park JC, Fishman GA, Collison FT. Full-field electroretinography, pupillometry, and luminance thresholds in X-linked retinoschisis. *Invest Ophthalmol Vis Sci*. 2020;61:53.

19. Alexander KR, Barnes CS, Fishman GA. Characteristics of contrast processing deficits in X-linked retinoschisis. *Vision Res*. 2005;45:2095–2107.

20. Graham CH. *Vision and Visual Perception*. New York: John Wiley & Sons; 1965:vii, 637.

21. Graham CH, Bartlett NR. The relation of size of stimulus and intensity in the human eye: II. Intensity thresholds for red and violet light. *J Exp Psychol*. 1939;24:574–587.

22. Graham CH, Brown RH, Mote FA. The relation of size of stimulus and intensity in the human eye: I. Intensity thresholds for white light. *J Exp Psychol*. 1939;24:555–573.

23. Smith VC, Sun VC, Pokorny J. Pulse and steady-pedestal contrast discrimination: effect of spatial parameters. *Vision Res*. 2001;41:2079–2088.

24. Barlow HB. Temporal and spatial summation in human vision at different background intensities. *J Physiol*. 1958; 141:337–350.

25. Watson AB. *Temporal Sensitivity*. New York: John Wiley & Sons; 1986.

26. Alexander KR, Barnes CS, Fishman GA. High-frequency attenuation of the cone ERG and on-response deficits in X-linked retinoschisis. *Invest Ophthalmol Vis Sci*. 2001;42:2094–2101.

27. Alexander KR, Barnes CS, Fishman GA. Origin of deficits in the flicker electroretinogram of the cone system in X-linked retinoschisis as derived from response nonlinearities. *J Opt Soc Am A Opt Image Sci Vis*. 2001;18:747–754.

28. Alexander KR, Fishman GA, Grover S. Temporal frequency deficits in the electroretinogram of the cone system in X-linked retinoschisis. *Vision Res*. 2000;40:2861–2868.

29. Prenner JL, Capone A, Jr, Ciaccia S, Takada Y, Sieving PA, Trese MT. Congenital X-linked retinoschisis classification system. *Retina*. 2006;26:S61–S64.

30. Lesch B, Szabo V, Kanya M, et al. Clinical and genetic findings in hungarian patients with X-linked juvenile retinoschisis. *Mol Vis*. 2008;14:2321–2332.

31. Anastasakis A, McAnany JJ, Fishman GA, Seiple WH. Clinical value, normative retinal sensitivity values, and intrasession repeatability using a combined spectral domain optical coherence tomography/scanning laser ophthalmoscope microperimeter. *Eye (Lond)*. 2011;25:245–251.

32. Shaqiri A, Roinishvili M, Grzeczkowski L, et al. Sex-related differences in vision are heterogeneous. *Sci Rep*. 2018;8:7521.

33. McAnany JJ, Park JC, Fishman GA, Hyde RA. Contrast sensitivity and equivalent intrinsic noise in X-linked retinoschisis. *Transl Vis Sci Technol*. 2022;11:7.

34. Pan F, Swanson WH. A cortical pooling model of spatial summation for perimetric stimuli. *J Vis*. 2006;6:1159–1171.

35. Sloan L. Area and luminance of test object as variables in examination of the visual field by projection perimetry. *Vision Res*. 1961;1:121–128.

36. Rovamo J, Virsu V, Nasanen R. Cortical magnification factor predicts the photopic contrast sensitivity of peripheral vision. *Nature*. 1978;271:54–56.

37. Khuu SK, Kalloniatis M. Standard automated perimetry: determining spatial summation and its effect on contrast sensitivity across the visual field. *Invest Ophthalmol Vis Sci*. 2015;56:3565–3576.

38. Khuu SK, Kalloniatis M. Spatial summation across the central visual field: implications for visual field testing. *J Vis*. 2015;15:1–15.

39. Fellman RL, Lynn JR, Starita RJ, Snyder WB. Clinical importance of spatial summation in glaucoma. In: Heijl A, ed. *Perimetry Update 1988/1989*. Amsterdam: Kugler & Ghedini; 1989:313–324.

40. Mulholland PJ, Redmond T, Garway-Heath DF, Zlatkova MB, Anderson RS. Spatiotemporal summation of perimetric stimuli in early glaucoma. *Invest Ophthalmol Vis Sci*. 2015;56:6473–6482.

41. Redmond T, Garway-Heath DF, Zlatkova MB, Anderson RS. Sensitivity loss in early glaucoma can be mapped to an enlargement of the area of complete spatial summation. *Invest Ophthalmol Vis Sci*. 2010;51:6540–6548.

42. Hansen RM, Moskowitz A, Akula JD, Fulton AB. The neural retina in retinopathy of prematurity. *Prog Retin Eye Res*. 2017;56:32–57.

43. Hansen RM, Tavormina JL, Moskowitz A, Fulton AB. Effect of retinopathy of prematurity on scotopic spatial summation. *Invest Ophthalmol Vis Sci*. 2014;55:3311–3313.

44. Hansen RM, Moskowitz A, Tavormina JL, Bush JN, Soni G, Fulton AB. Temporal summation in children with a history of retinopathy of prematurity. *Invest Ophthalmol Vis Sci*. 2015;56:914–917.